

# The T-lock: automated compensation of radio-frequency induced sample heating

Sebastian Hiller · Haribabu Arthanari ·  
Gerhard Wagner

Received: 24 February 2009 / Accepted: 6 April 2009 / Published online: 12 May 2009  
© US Government 2009

**Abstract** Modern high-field NMR spectrometers can stabilize the nominal sample temperature at a precision of less than 0.1 K. However, the actual sample temperature may differ from the nominal value by several degrees because the sample heating caused by high-power radio frequency pulses is not readily detected by the temperature sensors. Without correction, transfer of chemical shifts between different experiments causes problems in the data analysis. In principle, the temperature differences can be corrected by manual procedures but this is cumbersome and not fully reliable. Here, we introduce the concept of a “T-lock”, which automatically maintains the sample at the same reference temperature over the course of different NMR experiments. The T-lock works by continuously measuring the resonance frequency of a suitable spin and simultaneously adjusting the temperature control, thus locking the sample temperature at the reference value. For three different nuclei,  $^{13}\text{C}$ ,  $^{17}\text{O}$  and  $^{31}\text{P}$  in the compounds alanine, water, and phosphate, respectively, the T-lock accuracy was found to be  $<0.1$  K. The use of dummy scan periods with variable lengths allows a reliable establishment of the thermal equilibrium before the acquisition of an experiment starts.

**Keywords** Temperature control · Calibration · Chemical shifts · NMR

## Introduction

Control and stabilization of the sample temperature are crucial for high-resolution NMR experiments, because the chemical shift is a physical property sensitive even to small temperature changes of tenths of a degree Kelvin (Ohnishi and Urry 1969; Wüthrich 1986; Baxter and Williamson 1997). In conventional NMR probes, the temperature control is achieved with a thermocouple located in the air stream that forms the temperature reservoir for the sample. A temperature stabilization with a precision of below 0.1 K is typically achieved in such setups (Farrar et al. 1990), but these external measurements fail to detect the true sample temperature. In many experiments, strong radio frequency (RF)-pulses induce heat inside the sample due to dielectric absorption and undetected temperature increases of several degrees K can be encountered (Wang and Bax 1993; Wider 1998).

Differential sample heating in a series of experiments causes difficulties for the analysis of the spectra. For example, in protein structure determination schemes, the side chain protons of proteins are often assigned using TOCSY-type experiments with many high-power RF-pulses and thus strong sample heating (Braunschweiler and Ernst 1983; Bax et al. 1990; Montelione et al. 1992). In contrast, the NOESY experiments which provide proton–proton distance information feature only few RF-pulses and cause thus little sample heating (Kumar et al. 1980; Ikura et al. 1990). The calculation of protein structures from these experiments depends on the correlation of the chemical shifts in both experiments, especially for large proteins with high numbers of resonances, and a proper correction of the temperature differences is thus of paramount importance (Güntert 1998). A common interactive way to correct for differential RF-heating in a series of

S. Hiller · H. Arthanari · G. Wagner (✉)  
Department of Biological Chemistry and Molecular  
Pharmacology, Harvard Medical School, 240 Longwood  
Avenue, Boston, MA 02115, USA  
e-mail: gerhard\_wagner@hms.harvard.edu

experiments is manual adjustment of the temperature control, by comparing 1D traces of the spectrum of interest to a reference spectrum (Wider 1998). Such a procedure is however error-prone, cumbersome and time-consuming and forbids itself for automated or high-throughput setups.

Highly accurate and precise measurements of the sample temperature can be achieved in a non-invasive way by using the temperature-dependence of the chemical shift of suitable nuclei as thermometers (Dickert and Hellmann 1980; Field et al. 1984; Hedin and Furo 1998; Quast et al. 1998; Sikorski et al. 1998; Saunavaara and Jokisaari 2006; Findeisen et al. 2007). This is being used in many practical applications, in particular to calibrate the temperature unit of the NMR probe upon installation (van Geet 1970; Bornais and Brownstein 1978; Levy et al. 1980; Ammann et al. 1982), to map the local temperature in steady and non-steady state conditions (Wimmer and Wider 2007), to detect thermal convection currents (Jerschow 2000), or to improve the temperature stabilization (Keiichiro 1991). However, since chemical shifts are not only dependent on the temperature, but also on other sample parameters, like the pH value, the salt concentration, etc., the measured chemical shifts can be interpreted as temperatures only for samples with an exactly defined composition, e.g., containing the pure thermometer substance in bulk. In samples with a non-standard chemical composition, this interpretation is not applicable.

Here, we suggest a method that achieves accurate and precise stabilization of the NMR sample temperature during the course of one or several NMR experiments of interest by a combination of (1) continuously measuring the resonance frequency of a suitable inert thermometer substance using either 1D FT NMR or frequency sweeping, (2) using these resonance data to generate dynamic temperature values for the control of the heater system, (3) using a thermocouple measurement in the air stream to achieve precision, (4) employing the automated procedure “MET” for a combined management of the experiments of interest and the generation of the temperature control signals. MET stands for “Management of Experiments and Temperature”. By using inter-experimental periods of variable length, the steady state is established individually for each experiment in a series of experiments, and the temperature can thus be kept at the same reference value for one or several different experiments in an automated fashion. The temperature stabilization with this method reaches an accuracy of 0.1 K. The accuracy of conventional non-interactive systems can be 5 K or larger for experiments with strong RF-heating (Wang and Bax 1993) and compared to these the method presented here thus represents a 50-fold accuracy improvement. In reference to the field-frequency lock that is commonly used to stabilize the static magnetic field of an NMR magnet against field

drift or other disturbances we call the device described here a “T-lock”.

### Description of the T-lock concept

The spectrometer setup for the T-lock is shown in Fig. 1. The NMR sample of interest contains a suitable inert T-lock substance Z with the T-lock nucleus L. An example for aqueous samples is  $Z = \text{H}_2\text{O}$  and  $L = {}^{17}\text{O}$ , but many other choices are possible as discussed below. If the nucleus L is not covered by the existing channels of the NMR spectrometer setup, an additional channel for the nucleus L is added. The resonance frequency of the nucleus L in the compound Z,  $\delta(L^Z)$ , is continuously measured using either 1D FT-NMR or frequency sweeping (Fig. 2). Due to its higher sensitivity, the preferred implementation is acquisition of a 1D FT-NMR spectrum of nucleus L and subsequent automated peak-picking. For the alternative implementation with frequency sweep NMR, the resonance frequency of L is detected by continuous scanning, using the same or a similar technology that is used for conventional field-frequency-locks (Kan et al. 1978; Wider 1998). The detected values for  $\delta(L^Z)$  are continuously transmitted to the main spectrometer computer, which stores and analyzes these data using the MET procedure, which derives a dynamic temperature control signal,  $T_{\text{dyn}}$ , for the heat controller and simultaneously manages the execution of dummy scans and acquisition of the experiments.

The MET procedure consists of three main phases R, D and E corresponding to Reference, Dummy scans and Experiment, respectively (Fig. 3). Its performance during

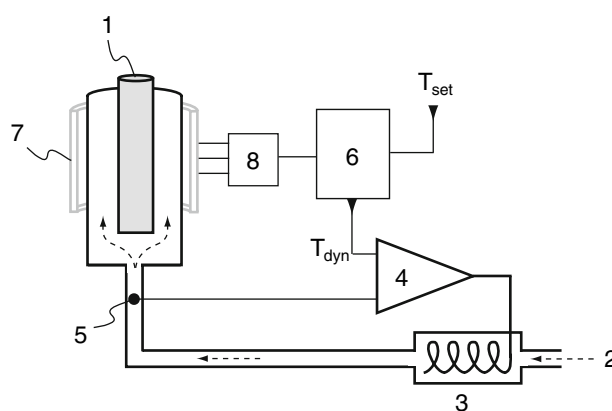


**Fig. 1** Block diagram of the T-lock setup. 1 Sample tube, sitting inside the NMR magnet. An air stream (dashed arrows) is provided by the air supply 2 and is heated by heater 3. 4 Controller for the heater, based on the temperature measured by thermocouple 5 and the dynamic temperature control value  $T_{\text{dyn}}$ . 6 Main computer. 7 Coils tunable to the resonance frequencies of all required nuclei. 8 NMR spectrometer containing channels for the required nuclei

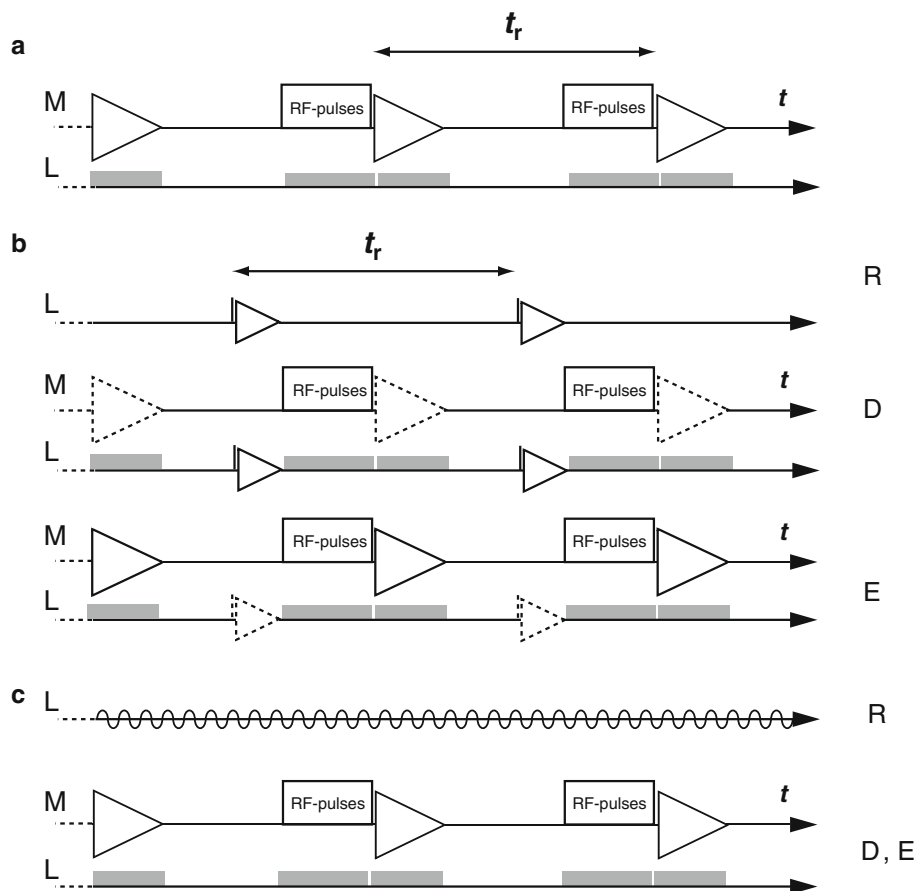


**Fig. 2** Resonance frequency measurement of the T-lock nucleus L. **a** Experimental scheme needed for the main experiment of interest. The RF-pulses are shown with open boxes. Recording of free induction decays (FID) is indicated with open triangles.  $t_r$  is the repetition time of the experiment. The same value for the repetition time is used in all panels of this figure. L represents the T-lock channel. M represents all other channels. The grey boxes denote pulse segments on nucleus L needed for the main experiment. **b** T-lock with 1D FT-NMR. The letters R, D, E denote the three phases of the MET procedure as defined in Fig. 3. R: Measurement of the reference value in the absence of any other experiment. A  $90^\circ$  pulse (bar) excites the steady-state magnetization of L with subsequent recording of an FID

(triangle). D: Pulse scheme during the dummy scans. The FID recordings on channel M (dashed triangles) are optional and are otherwise replaced by equivalent delays. E: Recording of the experiment. The acquisition of the T-lock frequency on channel L (dashed) is optional in this phase. **c** Embodiment of the T-lock with frequency sweeping. The letters R, D, E denote the three phases of the MET procedure. R: Measurement of the reference value in the absence of any other experiment. The frequency sweeping is indicated by wavy lines. D, E: Pulse scheme during the dummy scans and the experiment. Frequency sweeping is switched off during pulses on the nucleus L that are needed for the main experiment

two experiments is illustrated in Fig. 4. Phase R is initially executed once. With the heater control at  $T_{\text{set}}$ , the desired sample temperature chosen by the user, a reference value  $\delta_{\text{ref}}$  for  $\delta(L^Z)$  is recorded in the absence of other experiments. The sample heating caused by the pulses used to acquire  $\delta_{\text{ref}}$  can be neglected and the sample temperature is thus equal to the air stream temperature at this condition. In the implementation with 1D FT-NMR, the  $\delta_{\text{ref}}$  is acquired by a single scan of  $\delta(L^Z)$  or by the average of a number of scans defined by the user.

Phase  $D_i$  executes the dummy scans of experiment  $i$  and simultaneously measures  $\delta(L^Z)$ . The dummy scans induce the same amount of radio-frequency heating as the main experiment and thus the sample temperature changes by the

same amount as the main experiment. During the continuous execution of these dummy scans,  $T_{\text{dyn}}$  is adjusted by a suitable scheme until the chemical shift readings  $\delta(L^Z)$  match the reference  $\delta_{\text{ref}}$  acquired in phase R by a user defined tolerance. Once this steady-state condition is reached, the execution of the dummy scans is terminated and phase E, the regular acquisition of the experiment, is started. This transition is executed without an interruption of the pulse rhythm. If  $\delta(L^Z)$  is recorded,  $T_{\text{dyn}}$  can also be changed during the phase E. This can be important to compensate possible fluctuations of the air stream or for pulse sequences that change their RF-heating over the course of the experiment, e.g., if high-power decoupling is used during an indirect evolution time. Phases D and E are

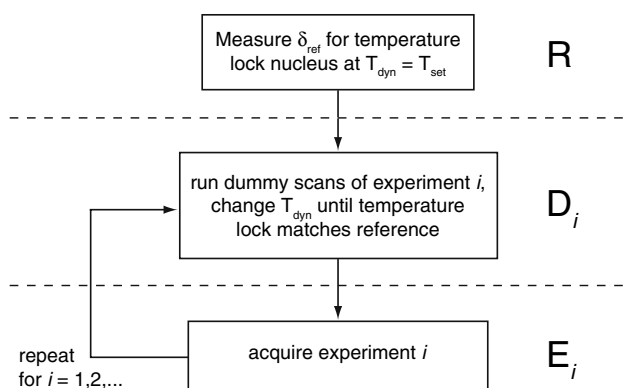


**Fig. 3** Overview of the MET procedure. The letters R, D, E refer to the three main phases Reference, Dummy scans, Experiment. The index  $i$  corresponds to the experiment number in a series of experiments. The dashed lines indicate the borders between the phases

executed once for each of multiple experiments until all scheduled experiments have been recorded. Typical lengths are 10–40 s for phase R, 10–500 s for phase D, and 10 min–10 d for phase E.

The chemical shift of the T-lock nucleus is referenced to the field-frequency lock. Thus, the effectively observed temperature shifts of  $\delta(L^Z)$  are a combination of the temperature shifts of the field-frequency lock resonance and the nucleus L in the substance Z. Thus, even nuclei that intrinsically have a weak or no temperature dependence can be suitable T-lock substances, if the field-frequency lock substance has a strong temperature dependence.

The accuracy of the T-lock, expressed in temperature intervals  $\Delta T$  that can unambiguously be distinguished, is estimated by

$$\Delta T \leq 2\sigma(\delta)c\sqrt{n}\left(\frac{\partial\delta}{\partial T}\right)^{-1} \quad (1)$$

where  $\sigma(\delta)$  is the precision of the  $\delta(L^Z)$  chemical shift measurement in a single scan,  $c$  specifies the width of the desired confidence interval resulting from a Gaussian distribution (e.g.,  $c = 4$  corresponds to 99.99% confidence),  $\partial\delta/\partial T$  is the temperature coefficient of the T-lock substance relative to the field-frequency lock, and  $n$  is the number of consecutive measurements which are averaged.

## Materials and methods

Measurements with  $^{13}\text{C}$  as T-lock substance were made with a sample of 50 mM [ $U\text{-}^{13}\text{C}$ ]-Alanine and 50 mM Arginine in 25 mM phosphate buffer, pH 6.8, [7%  $^2\text{H}$ ]- $\text{H}_2\text{O}$  on a Bruker Avance spectrometer operating at 500 MHz  $^1\text{H}$  frequency with a room temperature z-Gradient triple resonance probe. Measurements with  $^{17}\text{O}$  and  $^{31}\text{P}$  as T-lock substance were made with a sample of 50 mM phosphate buffer in [5%  $^{17}\text{O}$ , 7%  $^2\text{H}$ ]- $\text{H}_2\text{O}$  on a Varian 400 MHz spectrometer with a room temperature broad band detection probe. For all experiments, the static  $B_0$  field was locked using the  $^2\text{H}$  nucleus of  $\text{D}_2\text{O}$ . The chemical shift scales for all nuclei were defined by arbitrarily setting the field-frequency lock resonance of  $\text{D}_2\text{O}$  to 4.7 ppm at all temperatures and referencing all other nuclei indirectly to this fixed point by their relative gyromagnetic ratios (Wishart et al. 1995).

The 1D NMR spectra for temperature detection were recorded with a  $90^\circ$  excitation pulse followed by FID acquisition. 256, 11270, 1024 complex points were

**Fig. 4** Illustration of the functioning of the T-lock method during a typical setup. On the horizontal axis from left to right, time increases. Vertical dotted lines mark equal time points. **a** The periods R, D, E of the MET procedure, as defined in Fig. 3. **b** Chemical shift of the T-lock nucleus,  $\delta(L^Z)$ . The dashed horizontal line indicates  $\delta_{\text{ref}}$  as determined during phase R. **c** Dynamic temperature control settings,  $T_{\text{dyn}}$ , resulting from the MET procedure. The dashed horizontal line is the temperature  $T_{\text{set}}$  desired by the user

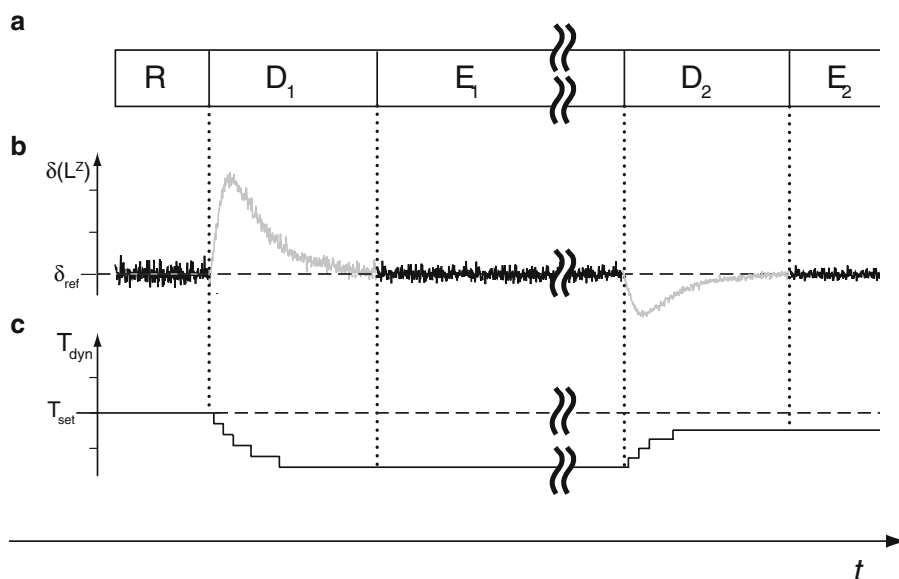
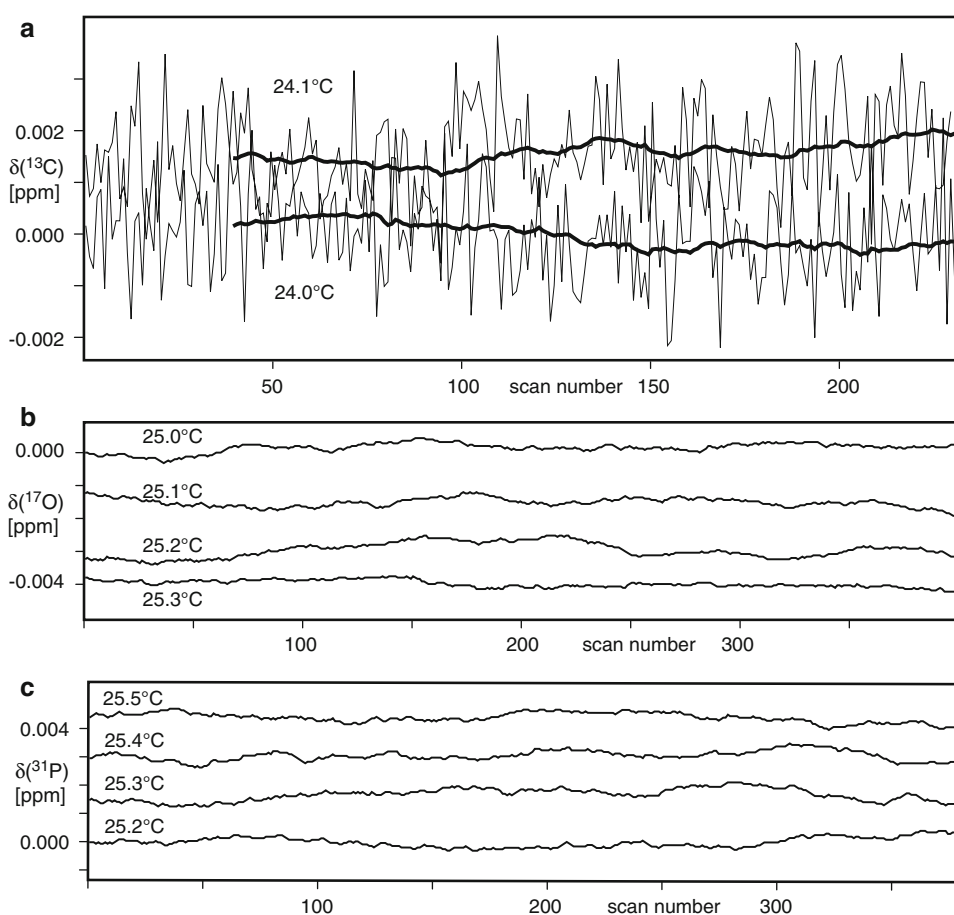


**Fig. 5** Stability curves of three T-lock substances in aqueous solution. **a**  $^{13}\text{C}$ -alanine, **b**  $^{17}\text{O}$ -water, **c**  $^{31}\text{P}$ -phosphate. The absolute temperatures are indicated next to each data set. Each scan is a 1D FT-NMR experiment followed by automated peak picking. In **(a)** the individual scans (thin lines) are shown in addition to the gliding average of 40 scans (bold lines). In **(b)** and **(c)**, the gliding averages of 40 scans are shown



recorded in 400, 1000, 61 ms for  $^{13}\text{C}$ ,  $^{31}\text{P}$ ,  $^{17}\text{O}$ , respectively. This interscan delay was adjusted to result in a repetition time of 1 s. The signal was zero-filled to 32 k complex points, multiplied with a cosine window function and Fourier transformed. From the 1D spectrum of  $^{13}\text{C}$ -alanine, one resonance line from the multiplet of the  $\text{C}^\beta$  atom at about 19 ppm was selected. The position of the peak maximum was interpolated from the intensity of the maximum and its two neighboring points by a peak picking algorithm (Hiller et al. 2008). The 1D spectra of  $^{17}\text{O}$ -water and  $^{31}\text{P}$ -phosphate featured exactly one resonance line each and in these experiments the global maximum was picked without interpolation.

2D [ $^{15}\text{N}$ ,  $^1\text{H}$ ]-HSQC experiments with  $^{13}\text{C}$ -decoupling during  $t_1$  were recorded using the pulse sequence of Wang and Bax, but without compensatory RF-irradiation outside (Wang and Bax 1993) with a 1 mM sample of the GB1 domain (Gronenborn et al. 1991) in 200 mM NaCl at pH 6.5 and 50 mM [ $U$ - $^{13}\text{C}$ ]-Alanine as the T-lock substance. The desired reference temperature was 25°C and the experiments were recorded on a Bruker Avance spectrometer operating at 500 MHz  $^1\text{H}$  frequency with a room temperature z-Gradient triple resonance probe.  $^{13}\text{C}$  broadband decoupling with GARP (Shaka et al. 1985) was

achieved with a 5 kHz  $\gamma\text{B}_1$  field. For the temperature correction,  $T_{\text{set}}$  was decreased by 0.1 K per 5.5 ms of  $t_1$ . The 2D spectra were recorded with  $t_{1,\text{max}} = 140$  ms.

## Results

Following Eq. 1, we evaluated the obtainable accuracy for the T-lock for three different nuclei in different lock compounds. The water chemical shift change is 10.3 ppb/K (Hartel et al. 1982; Cavanagh et al. 1996) and we observed effective chemical shift changes of about 20 ppb/K for  $^{13}\text{C}$ -alanine, 10 ppb/K for  $^{31}\text{P}$ -phosphate, and  $-10$  ppb/K for  $^{17}\text{O}$ -water on their respective frequency scales (Fig. 5). In order to distinguish steps of  $\Delta T = 0.1$  K with  $^{13}\text{C}$ -alanine as T-lock substance in a single scan, the chemical shift needs to be measured with a precision of 0.25 ppb or less (Eq. 1). In the presently tested setup, we find the precision to be about 1 ppb and averaging over 16 or more scans thus yielded the desired accuracy. Similarly, we could unambiguously distinguish 0.1 K steps for  $^{31}\text{P}$ -phosphate and  $^{17}\text{O}$ -water. Currently, we have not attempted to further optimize the obtainable accuracy below 0.1 K and these findings thus represent upper limits to the obtainable



accuracy, the amount of the lock substance and the number of averaged scans.

The most universal T-lock compound for aqueous solutions is  $^{17}\text{O}$ -water (see “Discussion”), but here we chose  $^{13}\text{C}$ -alanine to test the T-lock in a practical setup (Fig. 6) since this nuclei can be detected on a standard  $^1\text{H}$ ,  $^{13}\text{C}$ ,  $^{15}\text{N}$ -triple-resonance probe. In this example, a 2D [ $^1\text{H}$ ,  $^1\text{H}$ ]-TOCSY experiment with strong RF-heating increased the effective sample temperature by 2.3 K, inducing large chemical shift changes of the resonance frequency of the T-lock nucleus, which are corrected by the T-lock. By a comparison of the resonance positions of the first scan of the 2D [ $^1\text{H}$ ,  $^1\text{H}$ ]-TOCSY experiment with the 1D  $^1\text{H}$ -NMR reference spectrum at the reference temperature, which were virtually identical (Fig. 6b), we found that the temperature calibration obtained using the T-lock method to be highly accurate.

It is interesting to explore the possibilities of the T-lock to compensate for RF-periods with variable length in a multidimensional experiment. Such a case occurs for example in a 2D [ $^{15}\text{N}$ ,  $^1\text{H}$ ]-HSQC with  $^{13}\text{C}$ -broadband decoupling during  $t_1$ . During the course of the experiment, the  $t_1$  evolution time is increased, resulting in an increase of the sample temperature, causing teardrop-like peak shapes (Wang and Bax 1993) (Fig. 7b, d). A convenient method to correct for this effect is the addition of a compensatory RF-period outside the pulse scheme of interest, so that the overall RF-power is constant for each scan of the experiment (Wang and Bax 1993). As an alternative to the technique by Wang and Bax, the T-lock might be used to correct for the RF-induced heating. Since the T-lock is not fully implementable on current commercial spectrometers (see “Discussion”), we have explored this possibility indirectly. Monitoring the chemical shift of the T-lock compound  $^{13}\text{C}$ -alanine during the experiment shows that the sample temperature increase is roughly linear (Fig. 7a). To simulate the T-lock we then designed a linear gradient of  $T_{\text{set}}$  values, a decrease by 0.1 K per 5.5 ms of  $t_1$ , and the application of this gradient was found to compensate for the RF-induced temperature increase, leading to constant chemical shift of the T-lock (Fig. 7a). Consequently, application of this  $T_{\text{set}}$  gradient led to undistorted peak shapes in the 2D spectrum (Fig. 7c, e). We assume that the same or a similar  $T_{\text{set}}$  gradient would result from the real T-lock setup and thus conclude that the application of the T-lock for the compensation of temperature gradients during an experiment is in principle possible.

## Discussion

The T-lock should be beneficially applicable in a wide range of experimental situations. Depending on the sample

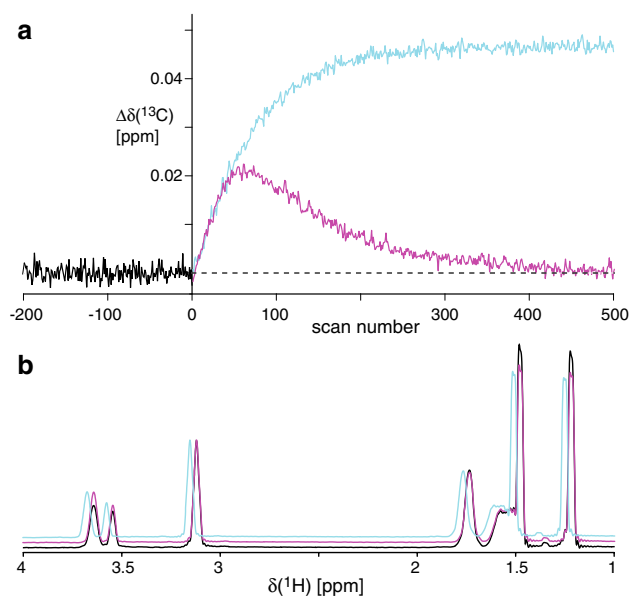
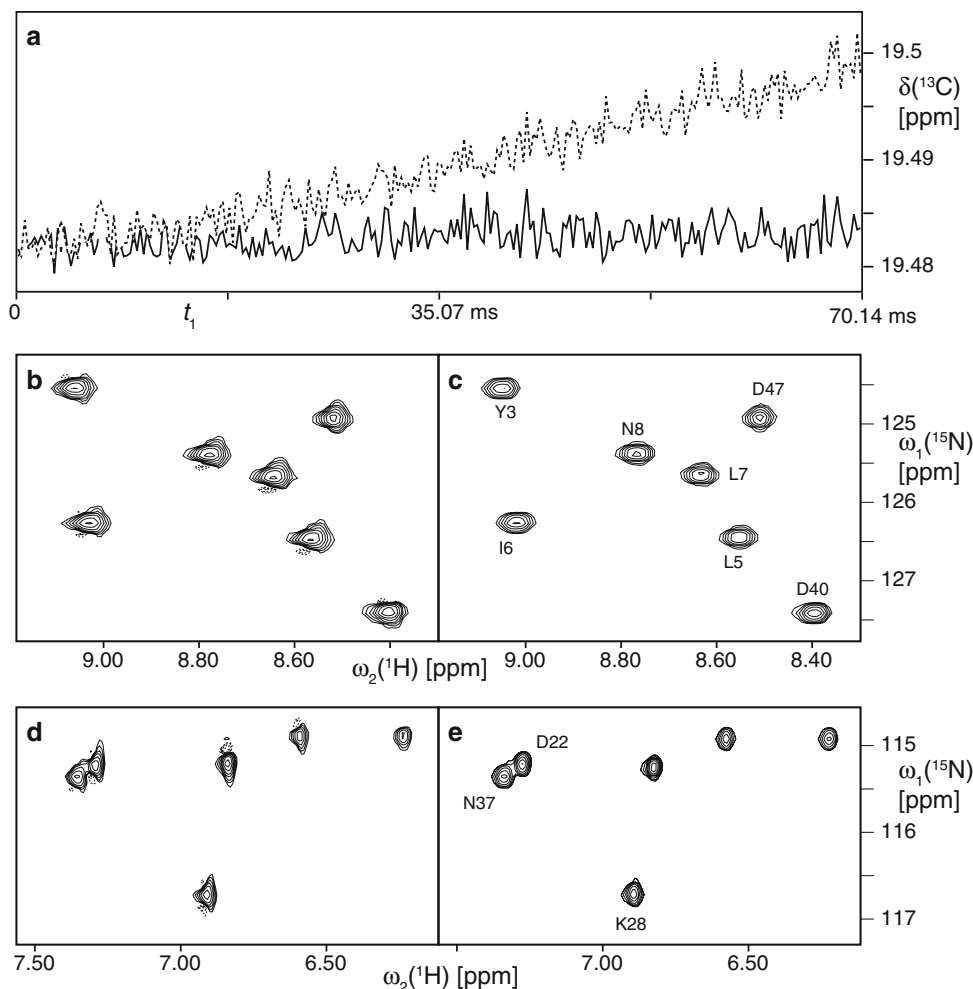


**Fig. 6** Application of the T-lock with a sample of 50 mM [ $U$ - $^{13}\text{C}$ ]-alanine and 50 mM arginine in aqueous solution in a representative experimental situation. **a** Resonance frequency of the T-lock nucleus  $^{13}\text{C}$  in the compound alanine. Black: 200 scans measured at the reference temperature of  $T_{\text{set}} = 25^\circ\text{C}$ . The average of 40 of these reference scans serves as the T-lock reference value  $\delta_{\text{ref}}$  (dashed horizontal line). Magenta/cyan: Resonance frequency of the T-lock nucleus during 500 dummy scans of a 2D [ $^1\text{H}$ ,  $^1\text{H}$ ]-TOCSY experiment with/without temperature adjustments by the MET procedure. **b** NMR spectra of the same sample in the same experimental situation. Black: 1D  $^1\text{H}$ -NMR spectrum at the reference temperature of  $T_{\text{set}} = 25^\circ\text{C}$ . Magenta/cyan: First scan of a 2D [ $^1\text{H}$ ,  $^1\text{H}$ ]-TOCSY experiment with/without using the T-lock, recorded directly after the corresponding dummy scans shown in **a**

composition, the choice of a suitable lock compound is guided by the following considerations. The main NMR experiment should not be impacted by the pulses required for the T-lock, and thus the nucleus L should be different from the nucleus, whose steady-state magnetization is used for the experiment of interest. The T-lock compound Z is ideally a small molecule with sharp resonance lines. It is also ideally a part of the desired sample preparation, so that no change in the chemical composition of the sample is required: preferably a nucleus from the solvent, such as  $^{17}\text{O}$ -water or  $^{13}\text{C}$ -labeled organic solvents or buffer components, such as  $^{31}\text{P}$ -phosphate, salts, organic buffer compounds, detergents or other additive molecules would be ideal. For protein samples in aqueous solution,  $^{13}\text{C}$ -labeled and perdeuterated amino acids, which can stabilize proteins, (Golovanov et al. 2004) or  $^{13}\text{C}$ -labeled 2,2-Dimethyl-2-silapentane-5-sulfonic acid (DSS) may also be T-lock compounds of choice. For biomolecular NMR, the use of  $^{13}\text{C}$  has the advantage that no channel needs to be added on conventional triple-resonance probes to implement the T-lock. On the other hand,  $^{17}\text{O}$  has the strong advantage of universal applicability on aqueous samples.

**Fig. 7** Application of the T-lock for the compensation of RF-heating with variable strength in a 2D experiment. **a** Chemical shift of the T-lock substance  $^{13}\text{C}$ -Ala during the recording of a 2D [ $^{15}\text{N}$ ,  $^1\text{H}$ ]-HSQC with  $^{13}\text{C}$ -broadband decoupling during  $t_1$ . The dashed line was recorded at fixed  $T_{\text{set}}$ . The solid line shows the same experiment with a linear  $T_{\text{set}}$  gradient applied (see text). **b–e** Two representative regions of the 2D [ $^{15}\text{N}$ ,  $^1\text{H}$ ]-HSQC spectrum of the protein domain GB1. **b, d** Spectrum recorded at fixed  $T_{\text{set}}$ , corresponding to the dashed line in **a**. **c, e** Spectrum recorded with a linear  $T_{\text{set}}$  gradient applied, corresponding to the solid line in **a**. Available resonance assignments are indicated, unassigned resonances correspond to side chains or unassigned backbone resonances. Note that the teardrop shape depends on the direction of the temperature-dependent shifts of the peaks in the 2D plane and is different in **b** and **d**



Using  $^{17}\text{O}$  may require an additional channel compared to triple-resonance probes, but it could also be possible that  $^{17}\text{O}$  can be detected via the same coil as deuterium, and the spectrum recorded by rapid receiver switching.

It is an important feature of the T-lock, that an absolute calibration of the temperature dependence of  $\delta(L^Z)$  is not required. After the reference signal is acquired, all the T-lock has to do is bring the resonance back to this reference value by changing the temperature setting  $T_{\text{dyn}}$ . Thus, not even a linear temperature dependence of  $\delta(L^Z)$  is a requirement. It is sufficient if the dependence is strictly monotonic.

In addition to stabilization of the temperature, the proposed method allows the transfer of the temperature calibration of a given sample to another spectrometer, since the same resonance frequency relative to the static field lock (in ppm) must be observed at the same temperature. This condition is true as long as the chemical composition of the sample is not changed and the parameters for the T-lock have been adjusted in a way to reproduce the same results on different spectrometers.

The T-lock measures the sample temperature as an average over the active volume of the sample and disregards possible temperature gradients along the sample, which are known to occur in different sizes depending on the probe geometry and other factors (Wimmer and Wider 2007). Strong temperature gradients can deteriorate the results of this method and need to be corrected by other engineering techniques.

Overall, the T-lock has the following advantages compared to other and conventional methods: (a) 50-fold improvement of the accuracy when compared to existing non-interactive methods (b) full automation when compared to interactive methods (c) acquisition of the experiments only when a thermal steady state is truly reached (d) direct transferability of a calibration on the same sample between different spectrometers. We thus believe that the T-lock would provide a useful tool to most NMR labs.

Unfortunately, an implementation as outlined here is currently not easily possible, since the interleaved acquisition of different nuclei on different channels and the proper data handling, data storage and control of the

temperature are not featured on commercially available spectrometers. Additionally, using the ideal compound for aqueous samples,  $^{17}\text{O}$ -water, may require a new type of probe design. However, in regard of the potential gains, we believe that implementing the necessary changes on soft- and hardware would be worth the effort. In addition to a strong simplification of data calibration, the T-lock should be very helpful for automated acquisition setups or for applications on multiple samples with possibly different dielectric properties, such as in metabonomics, where a comparison of high-resolution relies heavily on the temperature calibration. Importantly, the T-lock will facilitate automated approaches to protein structure determination.

**Acknowledgments** We thank Professor Philip H. Bolton for providing  $^{17}\text{O}$ -labeled water and Gregory Heffron and Charles Sheahan for help with the NMR measurements. This research was supported in part by NIH (grants GM47467, GM075879 and EB00206) and the Swiss National Science Foundation.

## References

- Ammann C, Meier P, Merbach AE (1982) A simple multinuclear NMR thermometer. *J Magn Reson* 46:319–321
- Bax A, Clore GM, Gronenborn AM (1990)  $^1\text{H}$ – $^1\text{H}$  correlation via isotropic mixing of  $^{13}\text{C}$  magnetization, a new 3-dimensional approach for assigning  $^1\text{H}$  and  $^{13}\text{C}$  spectra of  $^{13}\text{C}$ -enriched proteins. *J Magn Reson* 88:425–431
- Baxter NJ, Williamson MP (1997) Temperature dependence of  $^1\text{H}$  chemical shifts in proteins. *J Biomol NMR* 9:359–369
- Bornais J, Brownstein S (1978) A low-temperature thermometer for  $^1\text{H}$ ,  $^{19}\text{F}$ , and  $^{13}\text{C}$ . *J Magn Reson* 29:207–211
- Braunschweiler L, Ernst RR (1983) Coherence transfer by isotropic mixing—application to proton correlation spectroscopy. *J Magn Reson* 53:521–528
- Cavanagh J, Fairbrother WJ, Palmer AGIII, Skelton NJ (1996) *Protein NMR Spectroscopy: principles and practice*. Academic Press, San Diego
- Dickert FL, Hellmann SW (1980) Chemical shift thermometer for phosphorous-31 nuclear magnetic resonance measurements. *Anal Chem* 52:996–998
- Farrar TC, Sidky E, Decatur JD (1990) An inexpensive precise gas flow temperature controller. *J Magn Reson* 86:605–612
- Field LD, Sternhell S, Veigel W (1984) A high-temperature thermometer for  $^{13}\text{C}$  NMR spectroscopy. *Org Magn Reson* 22:221–223
- Findeisen M, Brand T, Berger S (2007) A  $^1\text{H}$ -NMR thermometer suitable for cryoprobes. *Magn Reson Chem* 45:175–178
- Golovanov AP, Hautbergue GM, Wilson SA, Lian LY (2004) A simple method for improving protein solubility and long-term stability. *J Am Chem Soc* 126:8933–8939
- Gronenborn AM, Filpula DR, Essig NZ, Achari A, Whitlow M, Wingfield PT, Clore GM (1991) A novel, highly stable fold of the immunoglobulin binding domain of streptococcal protein G. *Science* 253:657–661
- Güntert P (1998) Structure calculation of biological macromolecules from NMR data. *Q Rev Biophys* 31:145–237
- Hartel AJ, Lankhorst PP, Altona C (1982) Thermodynamics of stacking and of self-association of the dinucleoside monophosphate  $m_2^6\text{A-U}$  from proton NMR chemical shifts: differential concentration temperature profile method. *Eur J Biochem* 129:343–357
- Hedin N, Furo II (1998) Temperature imaging by  $^1\text{H}$  NMR and suppression of convection in NMR probes. *J Magn Reson* 131:126–130
- Hiller S, Wider G, Wüthrich K (2008) APSY-NMR with proteins: practical aspects and backbone assignment. *J Biomol NMR* 42:179–195
- Ikura M, Kay LE, Tschudin R, Bax A (1990) Three-dimensional NOESY-HMQC spectroscopy of a  $^{13}\text{C}$ -labeled protein. *J Magn Reson* 86:204–209
- Jerschow A (2000) Thermal convection currents in NMR: flow profiles and implications for coherence pathway selection. *J Magn Reson* 145:125–131
- Kan S, Gonord P, Fan M, Sauzade M, Courtieu J (1978) Automatic NMR field-frequency lock-pulsed phase locked loop approach. *Rev Sci Instrum* 49:785–789
- Keiichiro H (1991) Patent application 3-156394, Japan
- Kumar A, Ernst RR, Wüthrich K (1980) A two-dimensional nuclear Overhauser enhancement (2D NOE)-experiment for the elucidation of complete proton–proton cross-relaxation networks in biological macromolecules. *Biochem Biophys Res Commun* 95:1–6
- Levy GC, Bailey FT, Wright DA (1980) A sensitive NMR thermometer for multinuclei FT NMR. *J Magn Reson* 37:353–356
- Montelione GT, Lyons BA, Emerson SD, Tashiro M (1992) An efficient triple resonance experiment using carbon-13 isotropic mixing for determining sequence-specific resonance assignments of isotopically enriched proteins. *J Am Chem Soc* 114:10974–10975
- Ohnishi M, Urry DW (1969) Temperature dependence of amide proton chemical shifts—secondary structures of gramicidin S and valinomycin. *Biochem Biophys Res Commun* 36:194–202
- Quast H, Heubes M, Dunger A, Limbach HH (1998) A high-precision carbon-13 shift thermometer for the temperature range 100–300 K. *J Magn Reson* 134:236–244
- Saunavaara J, Jokisaari J (2006) Determination of sample temperature and temperature stability with  $^{129}\text{Xe}$  NMR. *J Magn Reson* 180:58–62
- Shaka AJ, Barker PB, Freeman R (1985) Computer-optimized decoupling scheme for wideband applications and low-level operation. *J Magn Reson* 64:547–552
- Sikorski WH, Sanders AW, Reich HJ (1998) Tris(trimethylsilyl)methane as an internal  $^{13}\text{C}$  NMR chemical shift thermometer. *Magn Reson Chem* 36:S118–S124
- van Geet AL (1970) Calibration of methanol nuclear magnetic resonance thermometer at low temperature. *Anal Chem* 42:679–680
- Wang AC, Bax A (1993) Minimizing the effects of radio-frequency heating in multidimensional NMR experiments. *J Biomol NMR* 3:715–720
- Wider G (1998) Technical aspects of NMR spectroscopy with biological macromolecules and studies of hydration in solution. *Prog Nucl Magn Reson Spectrosc* 32:193–275
- Wimmer R, Wider G (2007) Real-time imaging of the spatial distribution of rf-heating in NMR samples during broadband decoupling. *J Magn Reson* 187:184–192
- Wishart DS, Bigam CG, Yao J, Abildgaard F, Dyson HJ, Oldfield E, Markley JL, Sykes BD (1995)  $^1\text{H}$ ,  $^{13}\text{C}$  and  $^{15}\text{N}$  chemical-shift referencing in biomolecular NMR. *J Biomol NMR* 6:135–140
- Wüthrich K (1986) *NMR of proteins and nucleic acids*. Wiley, New York